

How to cite: *Angew. Chem. Int. Ed.* **2023**, e202305165
doi.org/10.1002/anie.202305165

Upconverting Nanoparticles

Bilayer-Coating Strategy for Hydrophobic Nanoparticles Providing Colloidal Stability, Functionality, and Surface Protection in Biological Media

Alexandra Schroter, Carla Arnau del Valle, María J. Marín,* and Thomas Hirsch*

Abstract: The surface chemistry of nanoparticles is a key step on the pathway from particle design towards applications in biologically relevant environments. Here, a bilayer-based strategy for the surface modification of hydrophobic nanoparticles is introduced that leads to excellent colloidal stability in aqueous environments and good protection against disintegration, while permitting surface functionalization via simple carbodiimide chemistry. We have demonstrated the excellent potential of this strategy using upconversion nanoparticles (UCNPs), initially coated with oleate and therefore dispersible only in organic solvents. The hydrophobic oleate capping is maintained and a bilayer is formed upon addition of excess oleate. The bilayer approach renders protection towards luminescence loss by water quenching, while the incorporation of additional molecules containing amino functions yields colloidal stability and facilitates the introduction of functionality. The biological relevance of the approach was confirmed with the use of two model dyes, a photosensitizer and a nitric oxide (NO) probe that, when attached to the surface of the UCNPs, retained their functionality to produce singlet oxygen and detect intracellular NO, respectively. We present a simple and fast strategy to protect and functionalize inorganic nanoparticles in biological media, which is important for controlled surface engineering of nanosized materials for theranostic applications.

Introduction

Nanomaterials are attractive for tracking biomacromolecules not only because of their exceptional physicochemical properties but also since they are similar in size. Their high surface-to-volume ratio is beneficial for functionalization with receptors, sensors, or drugs.^[1] At the same time, this feature bears the greatest challenge of nanomaterials, as it comes along with a high tendency of agglomeration.^[2] Thus, functionalization strategies are desirable that protect particles from agglomeration in biological environments and still allow the particle surface to be modified with different molecules in a targeted manner.^[3]

Upconversion nanoparticles (UCNPs) convert low-energy near-infrared (NIR) light into higher-energy visible or UV light. They typically consist of NaYF₄ host lattices doped with trivalent lanthanide ions. In most cases, a system

of two lanthanide ions is used, a sensitizer ion with strong NIR-absorption (e.g., Yb³⁺, Nd³⁺) and an activator ion that has a variety of energy levels, which are populated by the sequential absorption of more than one photon (e.g., Er³⁺, Tm³⁺, Ho³⁺). The transfer of the energy of two or more photons from the sensitizer ions to an activator ion enables the upconversion process.^[4] High temperatures are required to form hexagonal, monodisperse UCNPs, therefore synthesis protocols utilizing temperature-stable rare-earth-oleates in high boiling organic solvents have been established. Consequently, these oleate-stabilized particles are hydrophobic and therefore dispersible only in organic solvents.^[5] The same applies to many other nanosized probes, regardless of whether they are luminescent (e.g., quantum dots) or magnetic (e.g., superparamagnetic iron oxide particles). To date, many strategies have been proposed to elegantly facilitate transfer into an aqueous environment.^[6,7] UCNPs that are aimed for biomedical applications should exhibit colloidal stability and have the potential to be functionalized with receptors or reporter molecules, or with therapeutic agents.^[3] The simplest particle modification strategy is based on ligand exchange, in which the oleate is first removed in the presence of nitrosyl tetrafluoroborate or acid, while the desired ligand is added during a second modification step.^[8] This method has gained great popularity because of its capability to use a wide variety of ligands, ranging from small molecules to large polymers.^[9,10]

Despite the great charm of its simplicity, this method comes with a downside: it is almost impossible to adequately protect the surface of the particle through the ligand exchange, i.e., to cover it so completely that no further,

[*] A. Schroter, T. Hirsch
Institute of Analytical Chemistry, Chemo- and Biosensors, University of Regensburg
Universitätsstraße 31, 93053 Regensburg (Germany)
E-mail: thomas.hirsch@ur.de

C. Arnau del Valle, M. J. Marín
School of Chemistry, University of East Anglia
Norwich Research Park, Norwich NR4 7TJ (UK)
E-mail: M.Marin-Altava@uea.ac.uk

© 2023 The Authors. Angewandte Chemie International Edition published by Wiley-VCH GmbH. This is an open access article under the terms of the Creative Commons Attribution Non-Commercial License, which permits use, distribution and reproduction in any medium, provided the original work is properly cited and is not used for commercial purposes.

unwanted, binding of other molecules present in the solution is possible later. Molecules with functional groups such as $-\text{SO}_4$, $-\text{COOH}$, $-\text{NH}_2$ or $-\text{H}_2\text{PO}_3$ occupy free binding sites or even displace ligands, which can also lead to particle aggregation in addition to a changed functionality.^[10,11] Water molecules can diffuse to the weakly protected particle surface, which greatly impairs the upconversion effect due to quenching or disintegration effects.^[6,10,12,13] These drawbacks have been overcome with ligand modifications in which the oleate ligand remains on the particle surface and an amphiphilic coating, such as amphiphilic polymers, is added to aid water dispersibility while providing a hydrophobic barrier to protect the particle surface from quenching and dissolution.^[14] The preparation of such protected systems is usually time-consuming, as many parameters have to be carefully adjusted to prevent the polymer from unwanted cross-linking, potentially leading to particle aggregation.^[15] Alternatively, phospholipids can be used as amphiphiles to obtain biocompatible, bright, and colloidal stable UCNPs; however, this method is also laborious, expensive, and results often in low yield.^[16]

As an alternative, we present a fast and simple surface modification strategy that disperses nanoparticles in aqueous media, ensures bright upconversion luminescence as well as colloidal stability, and allows easy further functionalization (Figure 1). The procedure starts with oleate-coated UCNPs of any size between 10 and 50 nm dispersed in an organic solvent. The particles are then added to an aqueous suspension of sodium oleate and dodecylamine where, under mild conditions (1 h, 60 °C), the amphiphilic molecules interact with the hydrophobic alkyl chains on the particle surface forming a bilayer. The addition of dodecylamine in the bilayer formation allows for later functionalization.

Results and Discussion

Oleate-coated UCNPs (UCNPs@oleate) of the type $\text{NaYbF}_4(20\% \text{Er})/\text{NaYF}_4$ with a diameter of (23.3 ± 1.7) nm (Figures 2a and S1), were synthesized according to a previously published protocol.^[17] The UCNPs@oleate, initially dispersed in cyclohexane (31.2 mg mL^{-1}) were added

to an aqueous mixture of sodium oleate (50 mg mL^{-1}) and dodecylamine (15 mg mL^{-1} in DMSO). The transfer of the UCNPs@oleate from the organic phase to the aqueous phase took place within seconds as observed monitoring the upconversion luminescence upon excitation with a NIR handheld-laser. The initial slightly turbid solution became clear after evaporation of the cyclohexane, indicating that the particles were surrounded by the amphiphilic molecules and therefore were stable in the aqueous phase. In contrast, if UCNPs@oleate were added to water without the presence of amphiphilic molecules, the particles agglomerated and precipitated immediately. Following purification, the formation of a uniform bilayer is confirmed by transmission electron microscopy (TEM) images recorded on negatively stained grids (Figure 2b). A hydrodynamic diameter of (36.4 ± 0.6) nm (polydispersity index (PDI) = 0.147 ± 0.006) verifies that micelles with multiple individual particles were not formed (Figure 2c). High upconversion luminescence losses are usually observed when changing the solvent from organic to aqueous media.^[12] Here, 65 % of the upconversion luminescence of the UCNPs@oleate in cyclohexane was preserved after transfer to water (Figure 2d). In contrast, unprotected UCNPs (UCNPs@ BF_4^-) in water retained only 22 % of their original upconversion luminescence. This demonstrates the exceptional ability of the bilayer strategy to efficiently shield the particle surface from the solvent. To prove that this bilayer modification is also suitable for long-term storage, the particles were freeze-dried and characterized following redispersion in water. Dynamic light scattering (DLS) results confirmed that the UCNPs remained monodisperse (Figure S2). The UCNPs@bilayer exhibited a negative zeta potential of (-57 ± 4) mV and showed good colloidal stability in cell media and in the presence of high ionic strength (Figure S3). Under physiological conditions, significant agglomeration was only observed in the presence of high Ca^{2+} concentrations (1.8 mM). This is most likely due to the divalent character of the ion and the consequently stronger influence on the colloidal stability. In comparison to the also divalent Mg^{2+} , Ca^{2+} shows a weaker formation of hydrate shells and with this a higher reactivity towards counterions such as the oleate on the surface of the nanoparticles.^[18]

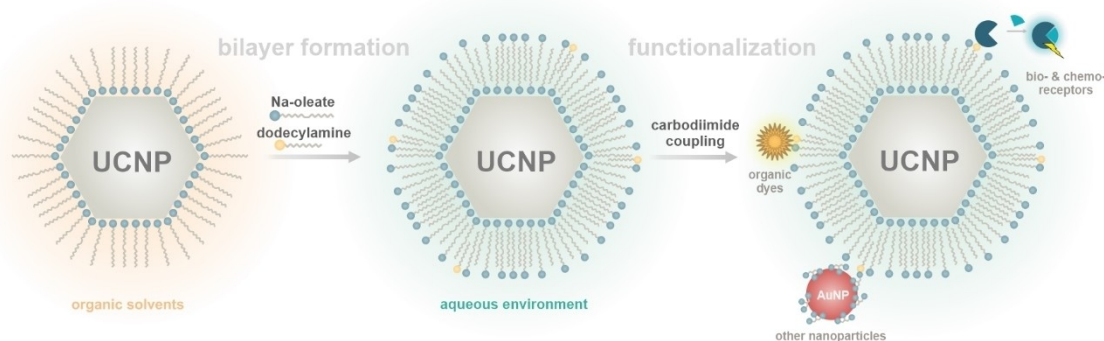


Figure 1. Particle modification strategy: transfer of oleate-capped UCNPs from a nonpolar environment into an aqueous environment by bilayer formation with the possibility of further functionalization.

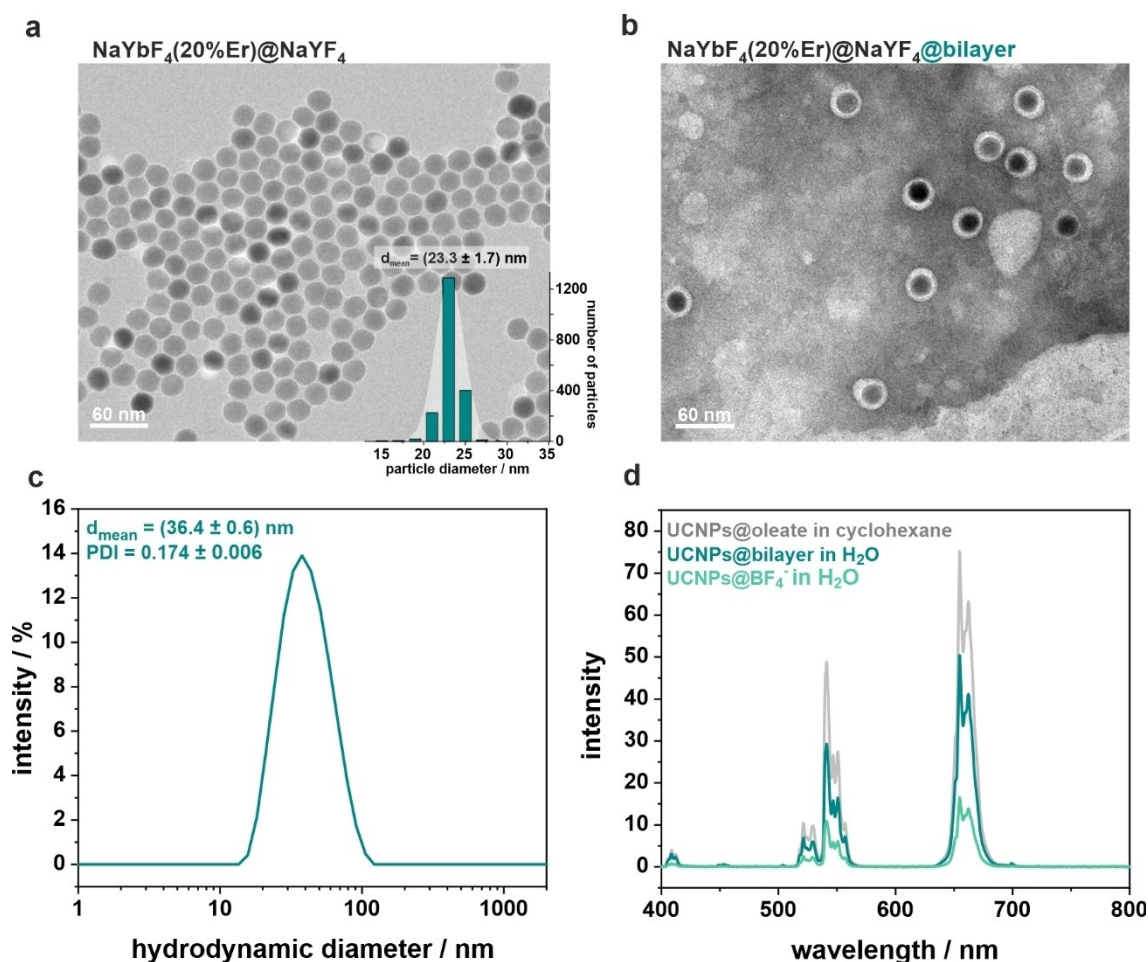


Figure 2. a) TEM image and corresponding particle-size-distribution of $\text{NaYbF}_4(20\% \text{Er})@ \text{NaYF}_4$ (UCNPs@oleate). b) TEM image of the same UCNPs after bilayer formation (UCNPs@bilayer). The TEM grid was negatively stained with phosphotungstic acid. c) DLS of UCNPs@bilayer in H_2O . d) Upconversion luminescence of UCNPs@oleate in cyclohexane, UCNPs@bilayer in H_2O and UCNPs@ BF_4^- in H_2O , where the oleate was removed via ligand exchange.^[6] All surface modifications shown were performed using the same batch of $\text{NaYbF}_4(20\% \text{Er})@ \text{NaYF}_4$, which were characterized in (a). Spectra ($\lambda_{\text{exc}} = 980 \text{ nm}$ at 140 W cm^{-2}) were normalized to the mass concentration determined by ICP-OES (for more details, see Supporting Information).

The incorporation of organic molecules is often required to introduce additional functionality to the particles and, consequently, improve their applicability. This should be achieved without losing colloidal stability. Since both carboxyl groups and amino groups are available on the UCNPs@bilayer, carbodiimide-coupling chemistry can be easily applied (Figure 3).

The coupling of a carboxyl group to the UCNPs was demonstrated using the photosensitizer Rose Bengal (RB) as model molecule. An RB-NHS-ester derivative was prepared and reacted with the UCNPs@bilayer (Figure 3, top). The particles were purified via centrifugation to remove unbound RB-NHS ester molecules.

Especially for FRET-based nanosystems, it is desirable to control the dye-loading of the UCNPs surface. The challenge is to find a compromise between sufficient signal intensities and self-quenching at too high concentrations. A plethora of surface modification strategies reported in the literature to date allow only little control of this property.^[19] In the case of bilayer modification, two strategies can be

followed to adjust the amount of dye: (1) varying the ratio of UCNPs:dye in the coupling protocol, or (2) controlling the ratio of sodium oleate:dodecylamine during bilayer formation. When attaching RB to the UCNPs, the possibility of controlling the amount of dye on the particle by varying the ratio of UCNPs to RB in the coupling step was confirmed by absorbance measurements (Figure 4). The colloidal stability of the particles was not affected by the attachment of the organic dye as only a slight increase in the hydrodynamic diameter was observed for the particles with the highest number of attached dye molecules (Figure S4a). When comparing the systems containing different amounts of RB, no clear difference in the luminescence measurements was observed under 980 nm excitation. In addition, the emission corresponding to RB at about 600 nm indicates radiative or non-radiative energy transfer from UCNPs to RB either via FRET or reabsorption (Figure S4b).

Different UCNPs@bilayer systems with varying percentages of dodecylamine (5%, 10%, 15%, 20%) and the respective added constant amount of activated RB were

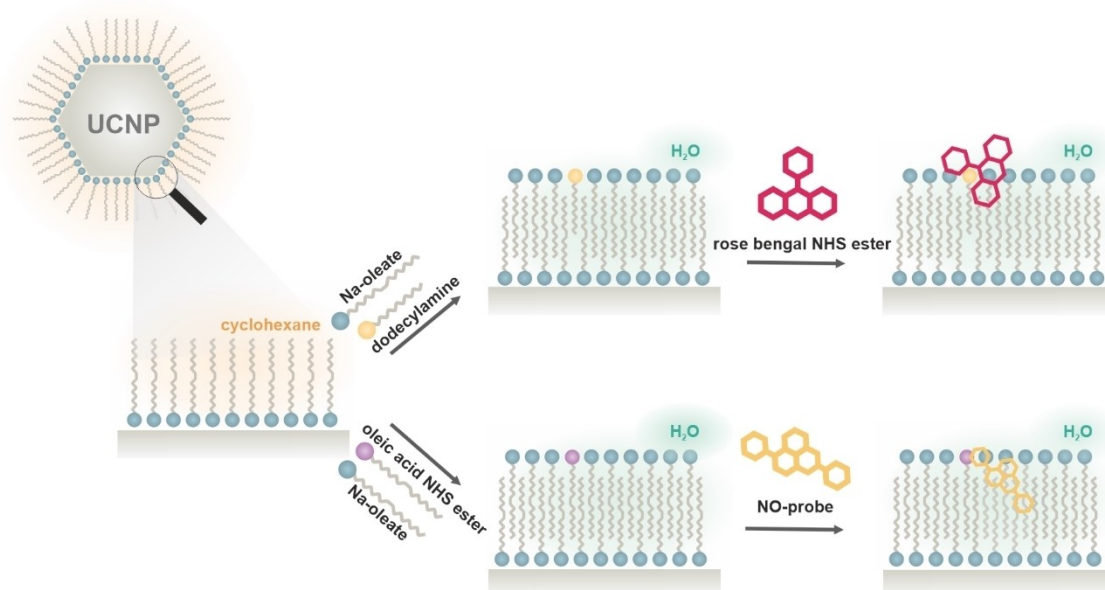


Figure 3. Carbodiimide-chemistry-based strategies for functionalization of UCNPs@bilayer with organic dyes containing a carboxy function (top) or an amino function (bottom).

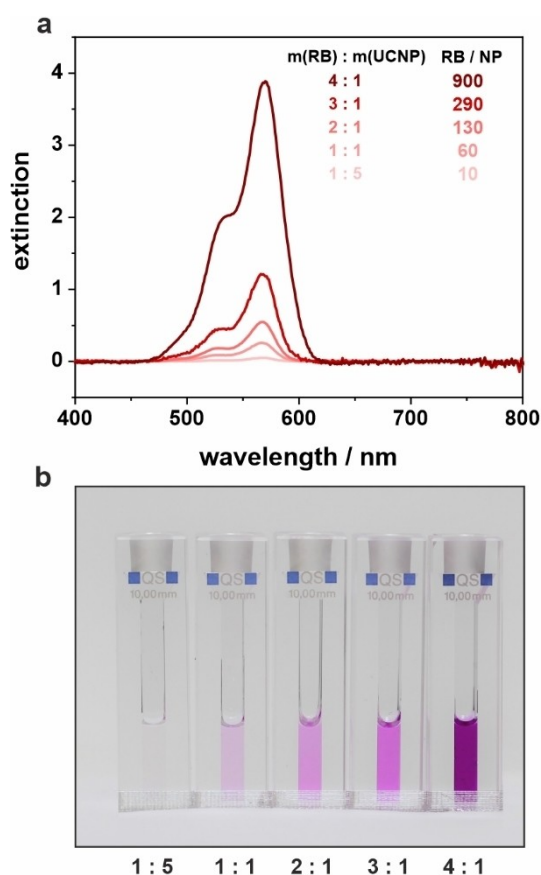


Figure 4. a) Extinction spectra and calculated number of RB molecules per nanoparticle of UCNPs@bilayer-RB with different ratios of $m(\text{RB}) : m(\text{UCNPs})$. The spectra are normalized to the mass concentration of UCNPs (1.0 mg mL^{-1}) as for some of the samples (4:1 and 3:1 dilution was required). b) UCNPs@bilayer-RB dispersions with different ratios of $m(\text{RB}) : m(\text{UCNPs})$.

synthesized to examine whether RB was covalently attached to the amine groups in the bilayer and not only intercalated between the amphiphilic molecules. The increase in the absorbance of RB with higher amounts of dodecylamine suggests that a binding of the dye to the amine groups is taking place (Figure S5a). These results also support that the degree of functionalization can be easily adjusted via the amine content in the bilayer. However, an optimal colloidal stability was found for UCNPs@bilayer with 10 mol % dodecylamine (Figure S5b).

The number of organic dyes and molecules with potential pharmacological properties that contain terminal amine groups is extensive, so expanding the application of the UCNPs@bilayer to support this type of molecule is paramount. As a proof-of-concept study, the bilayer was formed using activated oleate (oleate-NHS-ester) along with non-activated oleate and an amine derivative of the nitric oxide (NO)-sensitive dye DANPY-NO,^[20] referred to herein as the *NO-probe* (Figure 3, bottom). This two-photon excitable molecular probe has shown excellent performance for the detection of NO in a broad range of cells, including human macrophages and endothelial cells.^[20,21] The functionalization of UCNPs@bilayer with the *NO-probe*, motivated by the potential that a NIR-excitable ratiometric nanoprobe could have for biological applications, was achieved by a coupling reaction to previously carbodiimide-activated oleate molecules (1 mol % of total oleate) which were present during the bilayer formation. The resulting UCNPs@bilayer-*NO-probe* were characterized by a monodisperse size distribution with a hydrodynamic diameter of $(36 \pm 2) \text{ nm}$ (Figure S6a). A control experiment, in which a *NO-probe* was added to the reaction mixture without pre-activation of the oleate, resulted in unstable particles without labelling confirming the covalent interaction between the *NO-probe*

and the oleate (Figure S7). The UCNPs@bilayer-NO-probe exhibited the characteristic absorption maximum (Figure S6b), and fluorescence excitation (Figure S6c) and emission (Figure S6d) of the NO-probe, confirming the successful functionalization.

Since the oleate-based bilayer of the UCNP surface offers good protection against hydrophilic molecules and thus ions have a low affinity to diffuse through the hydrophobic barrier, biomolecules are unlikely to replace the oleate on the nanoparticle surface and induce nanoparticle aggregation. Additionally, electrostatic repulsions further stabilize the particles as indicated by the high zeta potentials of the systems (-44.5 ± 0.5 mV for UCNPs@bilayer-RB (see Figure S8 for full nanoparticle characterization) and -42.6 ± 0.6 mV for UCNPs@bilayer-NO-probe). To check the colloidal stability under biological conditions, these particle systems were dispersed in cell medium (DMEM +10% FCS) showing no agglomeration after 72 h (Fig-

ure S9) and demonstrating the applicability of such modified UCNPs under biological conditions.

The ability of UCNPs@bilayer-RB to generate singlet oxygen via indirect NIR excitation of the UCNPs was confirmed by the decrease in fluorescence emission intensity of the singlet oxygen probe 9,10-anthracenedipropionic acid (ADPA) upon 980 nm irradiation (Figure 5a). No singlet oxygen production was observed for the free RB when excited with NIR light, further indicating the energy transfer from the nanoparticles to the RB. The ability of the NO-probe to detect NO once bound to the surface of the UCNPs@bilayer particles was demonstrated using diethylamine NONOate as a NO donor. As expected, the fluorescence emission intensity of the probe increased in the presence of NO (Figure 5b). To further confirm the NO-sensing ability of the UCNPs@bilayer-NO-probe, their potential to monitor intracellular levels of NO was investigated.

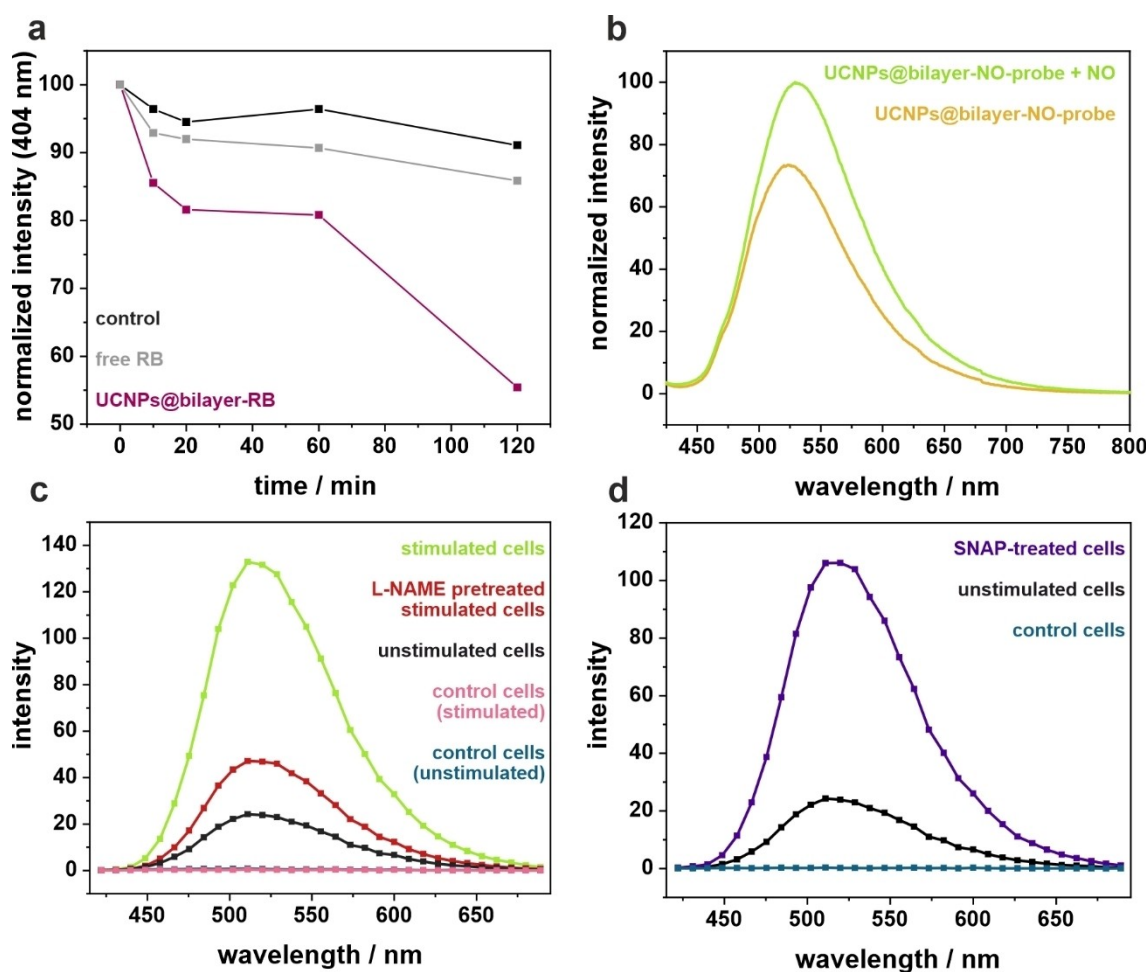


Figure 5. a) Singlet oxygen generation at different time periods of 980 nm irradiation detected by monitoring the fluorescence bleaching of ADPA excited at 390 nm. Normalized fluorescence decays of ADPA in the presence of UCNPs@bilayer-RB (pink), free RB (gray), and the corresponding control of only ADPA (black) in H₂O. b) Normalized fluorescence emission spectra of UCNPs@bilayer-NO-probe ($100 \mu\text{g mL}^{-1}$) before (yellow) and following (green) addition of NONOate (1.5 mM); $\lambda_{\text{exc}} = 405 \text{ nm}$. c) and d) Intracellularly recorded fluorescence emission spectra ($\lambda_{\text{exc}} = 405 \text{ nm}$) of RAW264.7 NO^- cells incubated with UCNPs@bilayer-NO-probe ($25 \mu\text{g mL}^{-1}$, 3 h) and treated under the following conditions: c) unstimulated (black), stimulated with LPS ($0.7 \mu\text{g mL}^{-1}$) and IFN- γ ($17 \mu\text{g mL}^{-1}$) (green) and pre-treated with L-NAME and stimulated with LPS ($0.7 \mu\text{g mL}^{-1}$) and IFN- γ ($17 \mu\text{g mL}^{-1}$) (red); and d) unstimulated (black), treated with SNAP ($275 \mu\text{M}$, 1 h, purple). Control unstimulated cells (blue in (c) and (d)) and control stimulated cells (pink in (c)) were also recorded.

As shown by confocal laser scanning microscopy images and corresponding intracellular spectra (Figure S10a and b, respectively), the nanoprobe was successfully internalized by RAW264.7 γ NO⁻ cells. The high cell survival rates at the concentrations tested indicated the great biocompatibility of the UCNPs@bilayer-NO-probe (Figure S10c). To evaluate the ability of the nanoprobe, which accumulated in the lysosomes of the tested cells (Figure S10d), to detect NO, two pathways of NO production in RAW264.7 γ NO⁻ cells were examined: endogenous and exogenous. NO was endogenously produced by RAW264.7 γ macrophages following stimulation with lipopolysaccharide (LPS) and interferon-gamma (IFN- γ), and exogenous NO was released by treating the cells with the NO-donor *S*-nitroso-*N*-acetylpenicillamine (SNAP). In both cases, strong intensity changes of the NO-probe fluorescence emission were observed in the presence of NO (Figure 5c and d, and Figure S11), suggesting that NO detection is indeed possible by the UCNPs@bilayer-NO-probe. Additionally, the selective detection of NO by the particles was proven using a NO synthase inhibitor (*N*(ω)-nitro-*L*-arginine methyl ester, L-NAME), which blocked the endogenous production of NO resulting in the decrease of the fluorescence emission intensity. This is the first indication that the bilayer coating is still intact, even after being taken up by biological cells.

The precise arrangement of the bilayer on the nanoparticle surface remains unclear since the incorporated amines appear to have an impact on the colloidal stability of the particles. This phenomenon was studied with different sized UCNPs and with different types of amines, which confirms that the stability is influenced by the presence and type of amine (Figure S12, Table S1). For example, for 23 nm particles, small hydrodynamic diameters and low PDIs were only observed for bilayer modifications including

10 mol % dodecylamine (Figure S12b). If no amine or other amines (octylamine, oleylamine) were incorporated into the bilayer, the particle size distributions indicated aggregate formation. The same effect was observed for smaller UCNPs (13 nm, Figure S12a), while the influence of the amine tends to become negligible for larger particles (Figure S12c). Comparing small and large UCNPs, it is known that small particles usually have a quasi-spherical shape and therefore large curvature, while the hexagonal prismatic shape usually evolves for larger particles.^[22] This shape changing effect is also evident by TEM studies (Figure S13). With regard to bilayer formation, a large curvature is disadvantageous because gaps can be expected between the oleate molecules.^[23] It is conceivable that the offered amine molecules fill the gaps and thus increase the stability of the UCNPs@bilayer. This is a phenomenon already known from cationic surfactant mixtures consisting of fatty acids and amines, which form extremely stable colloidal structures due to the decrease in the average ion head size and hence increasing packing parameters.^[24,25] For geometric and electrostatic reasons, these colloidal structures are strongly dependent on the chain length of the surfactant and the molar ratio anion:cation, which could explain the widely different results for the distinctive kind of amines.^[24] The stabilizing function of dodecylamine appears to be more important for small, highly curved particles. For larger UCNPs, the crystal edges are probably the most critical spots, as this is where a gap between the oleate molecules is to be expected. To verify this hypothesis, citrate-coated gold nanoparticles (AuNPs@citrate, 16 nm) were attached to 60 nm \times 48 nm UCNPs@bilayer via carbodiimide chemistry (Figure 6a). A clear tendency of the AuNPs to arrange predominantly on the edges than on the facets was observed in the TEM images. A control experiment with UCNPs@bi-

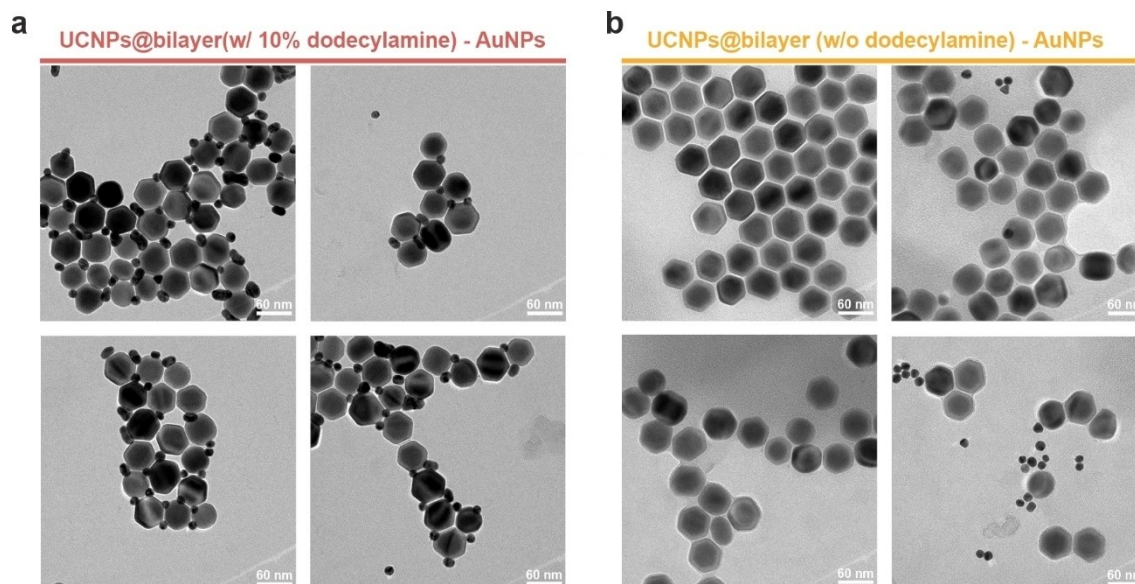


Figure 6. TEM images of UCNPs@bilayer (60 nm \times 48 nm) coupled to AuNPs@citrate (16 nm). a) UCNPs@bilayer with 10 mol% dodecylamine incorporated in the bilayer. b) Negative control of UCNPs@bilayer without dodecylamine in the bilayer and AuNPs treated under the same coupling protocol.

layer without amine showed no significant binding of AuNPs to the UCNPs, demonstrating the selective binding to the amine groups (Figure 6b). These results confirmed that the amines act as a gap filler stabilizing the bilayer.

Incorporation of 10 mol % dodecylamine is a reasonable choice for all particle sizes between 10 and 50 nm and is therefore recommended for bilayer modifications and functionalization. However, the ratio oleate:dodecylamine may need to be adjusted for very small (<10 nm) or very large (>50 nm) particles to address changes in the ratio of the total surface area to the total length of edges in the nanoparticle crystal. Furthermore, other amine-containing molecules, such as the NO-probe, can be also used to achieve stabilization via cationic electrostatic interaction.

Conclusion

The bilayer-strategy for simple surface modification and functionalization of hydrophobic nanoparticles yields hydrophilic and colloidally stable UCNPs. It was proven that dodecylamine has a positive, stabilizing function for the bilayer, which can be attributed to the positive effect of cationics on the stability of colloids but also due to a gap-filling function. It was demonstrated that the attachment of organic dyes to UCNPs@bilayer is possible in a very simple manner by carbodiimide coupling chemistry. Two proof-of-concept studies are shown: one where singlet oxygen was generated under 980 nm irradiation after attachment of RB to the UCNPs, and another, where a NO-sensitive probe was coupled to the particle surface to monitor exogenous and endogenous intracellular levels of NO. These results demonstrate that bilayer-coatings retain the functionality and allow their application for in vitro studies.

Supporting Information

The authors have cited additional references within the Supporting Information.^[17,21,26]

Acknowledgements

The authors would like to thank Susanne Märkl for the guidance in transmission electron microscopy, Sophia Baumann for support with photographic images and Patrick Recum for creating the cover image and his help in creating the graphical abstract (Institute of Analytical Chemistry, Chemo- and Biosensors, University of Regensburg). We also thank S.B. and P.R. for their help in vibrational spectroscopy. Furthermore, the authors thank Dr P. Thomas and Dr P. Wilson (Henry Wellcome Lab for Cell Imaging, Faculty of Science, University of East Anglia) for their guidance on imaging techniques. C.A.V. and M.J.M. would like to thank the Royal Society of Chemistry for financial support (Research Enablement Grant E21-2055114014). Open Access funding enabled and organized by Projekt DEAL.

Conflict of Interest

The authors declare no conflict of interest.

Data Availability Statement

The data that support the findings of this study are available from the corresponding author upon reasonable request.

Keywords: Fluorescent Probe · Interfaces · Lanthanides · Nanoparticles · Surface Chemistry

- [1] a) Y.-E. K. Lee, R. Smith, R. Kopelman, *Annu. Rev. Anal. Chem.* **2009**, *2*, 57; b) R. Lehner, X. Wang, S. Marsch, P. Hunziker, *Nanomedicine* **2013**, *9*, 742; c) P. Liu, R. Qin, G. Fu, N. Zheng, *J. Am. Chem. Soc.* **2017**, *139*, 2122.
- [2] C. Pfeiffer, C. Rehbock, D. Hühn, C. Carrillo-Carrion, D. J. de Aberasturi, V. Merk, S. Barcikowski, W. J. Parak, *J. R. Soc. Interface* **2014**, *11*, 20130931.
- [3] Y. Li, C. Chen, F. Liu, J. Liu, *Microchim. Acta* **2022**, *189*, 109.
- [4] a) M. Haase, H. Schäfer, *Angew. Chem. Int. Ed.* **2011**, *50*, 5808; b) X. Xie, N. Gao, R. Deng, Q. Sun, Q.-H. Xu, X. Liu, *J. Am. Chem. Soc.* **2013**, *135*, 12608; c) G. Chen, H. Qiu, P. N. Prasad, X. Chen, *Chem. Rev.* **2014**, *114*, 5161; d) Z. Zhang, S. Shikha, J. Liu, J. Zhang, Q. Mei, Y. Zhang, *Anal. Chem.* **2019**, *91*, 548.
- [5] a) H.-X. Mai, Y.-W. Zhang, R. Si, Z.-G. Yan, L. Sun, L.-P. You, C.-H. Yan, *J. Am. Chem. Soc.* **2006**, *128*, 6426; b) V. Muhr, C. Würth, M. Kraft, M. Buchner, A. J. Baeumner, U. Resch-Genger, T. Hirsch, *Anal. Chem.* **2017**, *89*, 4868.
- [6] S. Wilhelm, M. Kaiser, C. Würth, J. Heiland, C. Carrillo-Carrion, V. Muhr, O. S. Wolfbeis, W. J. Parak, U. Resch-Genger, T. Hirsch, *Nanoscale* **2015**, *7*, 1403.
- [7] L. Guerrini, R. A. Alvarez-Puebla, N. Pazos-Perez, *Materials* **2018**, *11*, 1154.
- [8] a) E. L. Rosen, R. Buonsanti, A. Llordes, A. M. Sawvel, D. J. Milliron, B. A. Helms, *Angew. Chem. Int. Ed.* **2012**, *51*, 684; b) A. Dong, X. Ye, J. Chen, Y. Kang, T. Gordon, J. M. Kikkawa, C. B. Murray, *J. Am. Chem. Soc.* **2011**, *133*, 998.
- [9] W. Kong, T. Sun, B. Chen, X. Chen, F. Ai, X. Zhu, M. Li, W. Zhang, G. Zhu, F. Wang, *Inorg. Chem.* **2017**, *56*, 872.
- [10] S. F. Himmelstoß, T. Hirsch, *Part. Part. Syst. Charact.* **2019**, *36*, 1900235.
- [11] L. Tong, E. Lu, J. Pichaandi, P. Cao, M. Nitz, M. A. Winnik, *Chem. Mater.* **2015**, *27*, 4899.
- [12] R. Arppe, I. Hyppänen, N. Perälä, R. Peltomaa, M. Kaiser, C. Würth, S. Christ, U. Resch-Genger, M. Schäferling, T. Soukka, *Nanoscale* **2015**, *7*, 11746.
- [13] a) O. Dukhno, F. Przybilla, V. Muhr, M. Buchner, T. Hirsch, Y. Mély, *Nanoscale* **2018**, *10*, 15904; b) S. Lahtinen, A. Lyytikäinen, H. Pääkkilä, E. Hömppi, N. Perälä, M. Lastusaari, T. Soukka, *J. Phys. Chem. C* **2017**, *121*, 656.
- [14] a) T. Pellegrino, L. Manna, S. Kudera, T. Liedl, D. Koktysh, A. L. Rogach, S. Keller, J. Rädler, G. Natile, W. J. Parak, *Nano Lett.* **2004**, *4*, 703; b) T. Černič, M. Koren, B. Majaron, M. Ponikvar-Svet, D. Lisjak, *Acta Chim. Slov.* **2022**, *69*, 448.
- [15] a) C.-A. J. Lin, R. A. Sperling, J. K. Li, T.-Y. Yang, P.-Y. Li, M. Zanella, W. H. Chang, W. J. Parak, *Small* **2008**, *4*, 334; b) S. Yang, N. Li, Z. Liu, W. Sha, D. Chen, Q. Xu, J. Lu, *Nanoscale* **2014**, *6*, 14903; c) M. Liras, M. González-Béjar, E. Peinado, L. Francés-Soriano, J. Pérez-Prieto, I. Quijada-Garrido, O. García, *Chem. Mater.* **2014**, *26*, 4014.
- [16] a) P. A. Rojas-Gutierrez, C. DeWolf, J. A. Capobianco, *Part. Part. Syst. Charact.* **2016**, *33*, 865; b) M. S. Meijer, V. S. Talens,

- M. F. Hilbers, R. E. Kiełtyka, A. M. Brouwer, M. M. Natile, S. Bonnet, *Langmuir* **2019**, *35*, 12079.
- [17] A. Schroter, S. Märkl, N. Weitzel, T. Hirsch, *Adv. Funct. Mater.* **2022**, *32*, 2113065.
- [18] a) S. E. Rodriguez-Cruz, R. A. Jockusch, E. R. Williams, *J. Am. Chem. Soc.* **1999**, *121*, 8898; b) R. Molinari, A. H. Avci, P. Argurio, E. Curcio, S. Meca, M. Plà-Castellana, J. L. Cortina, *J. Cleaner Prod.* **2021**, *328*, 129645.
- [19] a) S. Garbujo, E. Galbiati, L. Salvioni, M. Mazzucchelli, G. Frascotti, X. Sun, S. Megahed, N. Feliu, D. Prospero, W. J. Parak, et al., *Chem. Commun.* **2020**, *56*, 11398; b) J.-M. Montenegro, V. Grazu, A. Sukhanova, S. Agarwal, J. M. de La Fuente, I. Nabiev, A. Greiner, W. J. Parak, *Adv. Drug Delivery Rev.* **2013**, *65*, 677; c) K. E. Sapsford, W. R. Algar, L. Berti, K. B. Gemmill, B. J. Casey, E. Oh, M. H. Stewart, I. L. Medintz, *Chem. Rev.* **2013**, *113*, 1904.
- [20] C. Arnau del Valle, L. Williams, P. Thomas, R. Johnson, S. Raveenthiraraj, D. Warren, A. Sobolewski, M. P. Muñoz, F. Galindo, M. J. Marín, *J. Photochem. Photobiol. B* **2022**, *234*, 112512.
- [21] C. Arnau del Valle, P. Thomas, F. Galindo, M. P. Muñoz, M. J. Marín, *J. Mater. Chem. B* **2023**, *11*, 3387.
- [22] a) H.-X. Mai, Y.-W. Zhang, L. Sun, C.-H. Yan, *J. Phys. Chem. C* **2007**, *111*, 13730; b) X. Ye, J. E. Collins, Y. Kang, J. Chen, D. T. N. Chen, A. G. Yodh, C. B. Murray, *Proc. Natl. Acad. Sci. USA* **2010**, *107*, 22430.
- [23] J. Agudo-Canalejo, R. Lipowsky, *ACS Nano* **2015**, *9*, 3704.
- [24] A.-L. Fameau, T. Zemb, *Adv. Colloid Interface Sci.* **2014**, *207*, 43.
- [25] J. B. Engberts, J. Kevelam, *Curr. Opin. Colloid Interface Sci.* **1996**, *1*, 779.
- [26] a) L. Ludvíková, P. Friš, D. Heger, P. Šebej, J. Wirz, P. Klán, *Phys. Chem. Chem. Phys.* **2016**, *18*, 16266; b) S. Märkl, A. Schroter, T. Hirsch, *Nano Lett.* **2020**, *20*, 8620.

Manuscript received: April 12, 2023

Accepted manuscript online: May 30, 2023

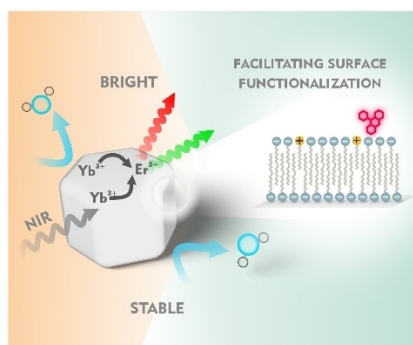
Version of record online: ■■, ■■

Research Articles

Upconverting Nanoparticles

A. Schroter, C. Arnau del Valle,
M. J. Marín,* T. Hirsch* — e202305165

Bilayer-Coating Strategy for Hydrophobic Nanoparticles Providing Colloidal Stability, Functionality, and Surface Protection in Biological Media



Modifying the surface of oleate-coated hydrophobic particles to render them stable in aqueous biological environments is often challenging. We present a one-step reaction, to form a bilayer consisting of oleate and dodecylamine moieties, which provides excellent stability and versatility as it allows further functionalization via carbodiimide chemistry.